Surface-imaging of frozen blue phases in a discotic liquid crystal with atomic force microscopy

Anton Hauser,[a] Mario Thieme,[a] Alfred Saupe,[a] Gerd Heppke*[b]† and Daniel Krüerke*[b]

[a]*Max-Planck-Arbeitsgruppe Flüssigkristalline Systeme an der Martin-Luther-Universität Halle, Mühlpforte 1, D-06108 Halle, Germany*

[b]*Iwan-N.-Stranski Institut für Physikalische und Theoretische Chemie, Sekr. ER11, Technische Universität Berlin, Strasse des 17. Juni 135, D-10623 Berlin, Germany*

Discotic cholesteric phases with extremely small pitches were obtained with cellobiose derivatives as chiral dopants. These binary mixtures tend to form up to three distinct blue phases. An interesting property of these mixtures is that the blue phases can be supercooled to a glass-like state. Microscopic studies, reflection spectra, and Kossel diagrams all indicate that the three discotic blue phases BP_DI, BP_DII and BP_DIII are analogous to the well-known calamitic modifications. In addition to the optical studies, we investigated the free surfaces of the frozen blue phases using atomic force microscopy.

Blue phases are formed by calamitic mesogens of a high chirality in a narrow temperature interval close to the clearing point. They have been studied intensively theoretically and experimentally.[1] Up to three blue phases can be distinguished. Two of these phases have a periodic orientational order that can be characterised by crystallographic space-group symmetries. The low temperature modifications BPI and BPII possess a cubic lattice symmetry with the space group $I4_132$ (O^8) and $P4_232$ (O^2), respectively. According to the theory of Meiboom *et al.*,[2] these structures can be described as a combination of double twist cylinders and disclinations (Fig. 1). Alternatively, a Landau theory has been developed by Hornreich and Shtrikman which shows that blue phases can be thermodynamically stable in certain regions of the temperature–chirality plane.[3] Blue phases are optically active but, unlike the cholesteric phase, they are optically isotropic and are not birefringent.[4]

The high temperature modification (BPIII) appears on cooling from the isotropic phase as an amorphous 'blue fog'. BPI, BPII and BPIII exhibit selective reflection of circularly polarised light and strong optical activity indicating a local helical structure with correlations over distances of the helical pitch.[5] But in contrast to BPI and BPII modifications, BPIII does not exhibit the Bragg scattering of a lattice structure. Its structure is not thoroughly understood and still subject to scientific discussion.[6,8]

A considerable amount of the ordering can occur at the isotropic–BPIII transition. For many compounds the major part of the latent heat in the phase sequence *cholesteric phase – blue phases – isotropic phase* is given off at the last transition.[7] Interestingly, the first-order BPIII–isotropic phase transition line can end at a critical point in highly chiral systems, as shown recently.[8] Assuming a one-to-one correspondence between the liquid–gas and the BPIII–isotropic phase transition, a theory of a critical point in the BPIII–isotropic phase diagram has been proposed by Lubensky and Stark.[9]

Freeze-fracture electron micrographs of BPIII appear to show a disordered packing of filamentary objects[10] confirming the 'spaghetti-model' of BPIII, in which the molecular arrangement can be described by a spaghetti-like tangle of double twist tubes.

Recently, we reported the first observation of discotic blue phases in binary mixtures of a discotic nematic host and chiral dopants.[11] Three blue phases could be observed for concentrations close to the solubility limit of the dopants. The textures of these modifications are very similar to the textures of the corresponding calamitic modifications.

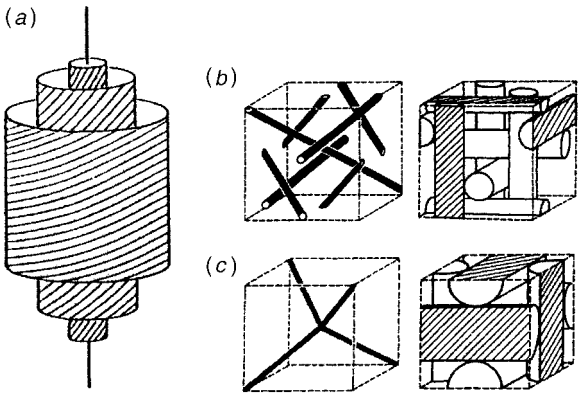

Fig. 1 (*a*) Schematic representation of a double twist cylinder (the lines represent orientation of the director). Arrangement of the disclination lines (left) and the double twist tubes (right) for (*b*) the unit cell of BPI and (*c*) the unit cell of BPII. (Figures from E. Dubois-Violette and B. Pansu.[12])

In order to investigate the complicated structure of the blue phases by scanning probe microscopy, some attempts were made for calamitic systems to freeze the structures into glass like states with chiral polymers, oligomers and networks.[13,14] With the low molar mass discotic mixtures under investigation it is possible, by rapid cooling, to obtain glassy states of the cholesteric phase and the blue phases BP_DI, BP_DII, and maybe even BP_DIII.[11] This allows the investigation of the periodic structure of BP_DI and BP_DII by the Kossel method at ambient temperature and atomic force microscopy of the free surfaces of blue phases and the cholesteric phase.

Materials

While the nematic phase N of rod-like molecules is very well known, the nematic phase N_D of disc-like molecules has been the subject of far fewer investigations. In contrast to the large number of calamitic liquid crystals, only a few discotic nematic compounds have been found so far. Many discotic mesogens tend to form the higher ordered columnar phases instead of the nematic phase.[15]

† Internet: www.tu-berlin.de/~insi/agheppke.html

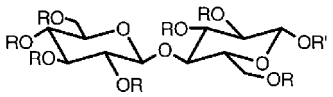

1 R = $COC_{10}H_{21}$, R' = $C_{11}H_{23}$

D_{ho} 93 °C Iso

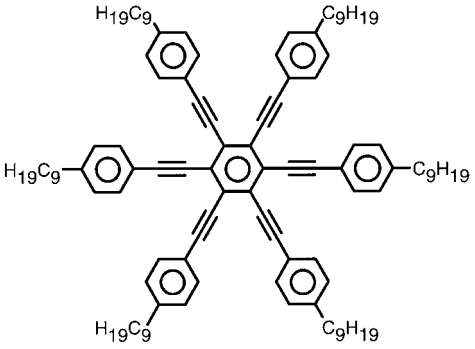

2 Cr 67 °C N_D 83 °C Iso

Fig. 2 Perlauroyl cellobioside **1**, the chiral dopant (Cr 47 D_{ho} 93 °C Iso) and hexakis[(4-nonylphenyl)ethynyl]benzene **2**, discotic nematic host system (Cr 66 N_D 83 °C Iso). For the blue phase samples we selected a binary mixture of 16 mass% of the chiral dopant **1** in the discotic nematic host **2** (N_D* 48.2 BP_DI 50.6 BP_DII 51.8 BP_DIII 52.6 °C Iso). Microscopic observations while heating reveals a glass transition at about 47 °C.

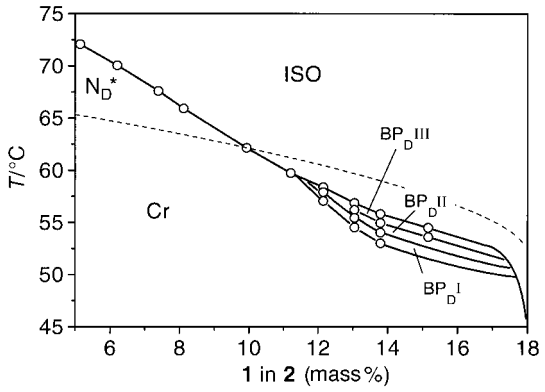

Fig. 3 Phase diagram of the investigated system, obtained using the contact method, complemented by the transition temperatures obtained for selected mixtures. The broken line is the melting curve; the solubility limit of the chiral dopand is about 20 mass%.

For our investigations the discotic cellobiose derivative **1** was used as chiral dopant, which was kindly provided by Dr Volkmar Vill from the University of Hamburg. The pure compound probably forms a columnar phase with nontilted hexagonal ordering. As the discotic nematic host we synthesized the hexakis[(4-nonylphenyl)ethynyl]benzene **2**. These kinds of 'multiyne' structures were developed about ten years ago in Berlin by Praefcke's group.[16] They form nematic phases at moderate temperatures.

The schematic phase diagram shown in Fig. 3 has been determined using a contact preparation and a number of discrete mixtures. It shows, at low concentrations of the chiral dopant, an enantiotropic discotic cholesteric phase, which exhibits a right-handed helical structure as determined by analysing the selectively reflected light of a shear aligned sample.

At higher concentrations of the chiral dopant, 12–17 mass%, the enantiotropic phase behaviour disappears, and is replaced by monotropic discotic blue phases and the discotic cholesteric phase.

The higher temperature blue phase appears as an amorphous

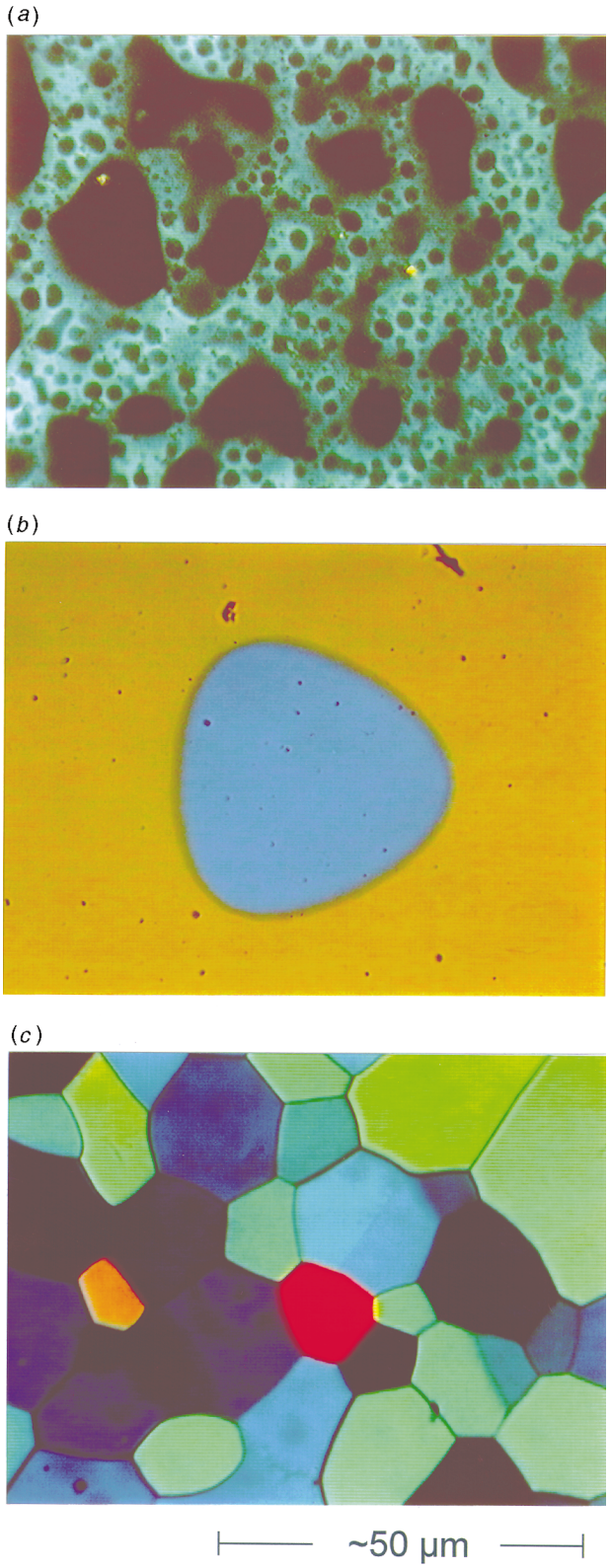

Fig. 4 Optical micrographs of (*a*) the discotic blue fog phase (BP_DIII), (*b*) a single crystal of the simple cubic BP_DII in the [111] orientation, and (*c*) the platelet texture of the body centred cubic modification BP_DI

blue haze on slow cooling from the isotropic liquid and is classified as being the BP_DIII or 'fog phase' [Fig. 4(*a*)].

Continued cooling of BP_DIII at low cooling rates (*i.e.* 0.2 °C min^{-1}) results in the appearance of a second and a third form of blue phase (BP_DII and BP_DI). Careful control of the temperature over periods of time can result in the growth of large and well-defined platelets [Fig. 4(*b*), (*c*)].

For our investigations we selected a binary mixture of 16

mass% of the chiral dopant **1** in the discotic nematic host **2** [phase sequence: Cr 60 °C (N_D* 48.2 BP_DI 50.6 BP_DII 51.8 BP_DIII 52.6 °C) Iso]. By rapid cooling (see Experimental) it was possible to solidify the textures of the monotropic blue phases. The microscopic observation of the vitrified liquid crystal texture while heating reveals a glass transition at *ca.* 47 °C. When slowly heating the sample, onset of crystallisation is observed under the microscope at *ca.* 50 °C. At *ca.* 3 °C below this temperature, the viscosity drops considerably, so that birefringence could be induced by shearing the sample. The glass transition could not be established by DSC measurements because of crystallization even at the fastest cooling rate.

Experimental

In order to prepare the samples for atomic force microscopy we spread the material on a glass slide and left the sample at the appropriate temperature on a Mettler-FP82 hot stage until a desired blue phase texture appeared. To freeze the phase we rapidly pressed the substrate onto a metal surface cooled with liquid nitrogen. The thickness of the samples obtained were 5–10 μm as revealed by AFM investigations.

Since the lattice constant of the blue phases is within the range of visible wavelength, Bragg reflection occurs in certain directions when the sample is illuminated with monochromatic divergent light. Kossel diagrams of the blue phase single crystals can be observed conoscopically (Fig. 5). All samples were investigated by this method prior to AFM investigations.

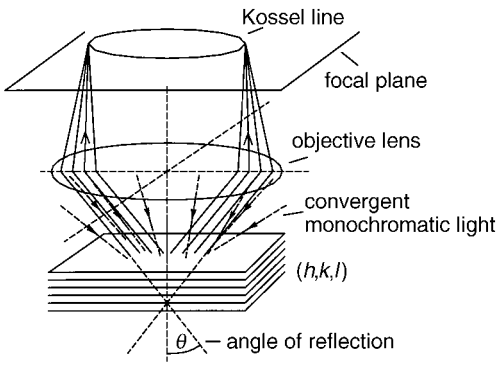

Fig. 5 Schematic procedure for Kossel diagrams. If blue phase single crystals are illuminated with convergent monochromatic light of wavelength λ, then the cosine of the angle of reflection θ from one set of planes (h,k,l) is given by eqn. (1) ($\bar{n}$ isotropic refractive index, a cubic lattice constant).

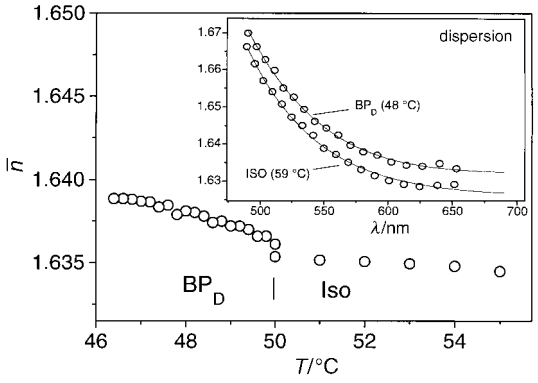

Fig. 6 The temperature dependence of the average refractive index at 589 nm as well as the dispersions determined by the Fabry–Perot method

Table 1 Selection rules for the simple cubic (sc) and the body centred cubic (bcc) structures

simple cubic (sc)	all *h, k, l*	100, 110, 111, 200,...
body centred cubic (bcc)	$h+k+l$=even	110, 200, 211, 220,...

Table 2 Kossel diagrams for the simple cubic (sc) and the body centred cubic (bcc) lattice structures when viewed along the indicated axes for decreasing wavelengths from top to bottom row (Kossel lines were calculated according to the description of Pieranski *et al.*[20])

[001]-orientation		[011]-orientation		[111]-orientation		
sc (BPII)	bcc (BPI)	sc (BPII)	bcc (BPI)	sc (BPII)	bcc (BPI)	*hkl*
						100
						100 110
						100 110 111
						100 110 111 200

The Kossel diagrams were recorded using an Ortholux II-Pol reflection microscope with an immersion objective lens (125×) and equipped with a CCD video camera and an ISA-

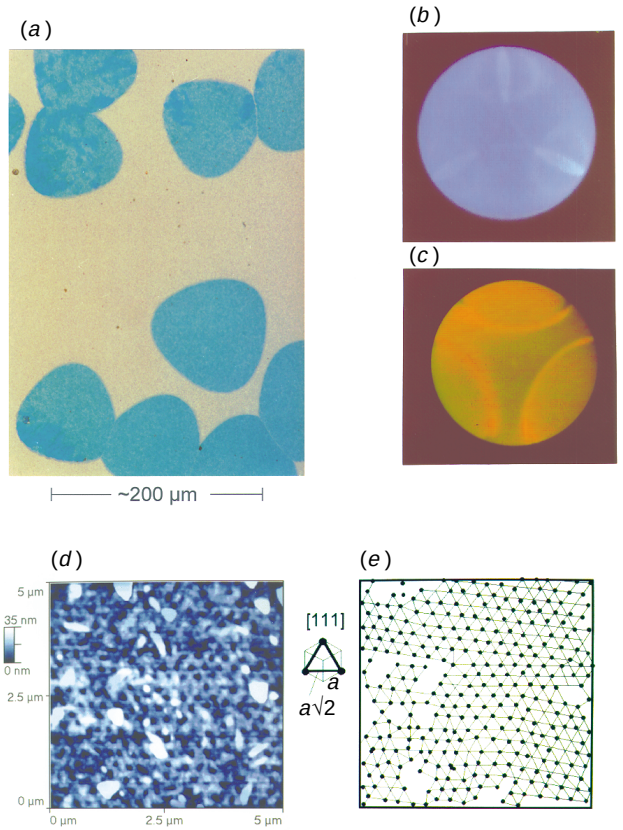

Fig. 7 (*a*) Optical micrograph of a frozen BP_DII single crystal between crossed polarizers in transmission, the corresponding Kossel diagrams at (*b*) λ=480 and (*c*) 560 nm and (*d*) the AFM surface pattern of that region. The underlying lattice structure emerges quite clearly in a drawing of the lattice points seen in the AFM image. The lattice constant was determined in three directions to be 208±8 nm and is in good agreement with the value obtained from the Kossel method (210±4 nm).

Monochromator (H 25). According to the optical selection rules (Table 1) the Kossel diagram yields information about the symmetry and the orientation of the blue phase lattice (Table 2). An overview and a general description of the Kossel method is given in a recent paper about the determination of the lattice parameters from blue phase Kossel diagrams.[17]

Each Kossel line observed in the focal plane of the microscope *via* a Bertrand lens represents one set of planes (h,k,l). The lattice constants a are obtained from the Bragg equation [eqn. (1)] inserting the wavelength λ where a Kossel line appears and the aperture angle θ is equal to zero.

$$a = \lambda \frac{\sqrt{h^2+k^2+l^2}}{2\bar{n}\cos\theta} \qquad (1)$$

The required average refractive index $\bar{n}$ of the blue phase was determined at a series of temperatures by observing the wavelength maxima of interference patterns of incident light in a transmissive mode and using a least-squares numerical analysis to calculate the ratio of optical path length of an empty cell (assuming $n_{air}=1$), d_0, to that of a cell filled with the sample, d_{BP} [eqn. (2)].

$$\text{Average refractive index, } \bar{n} = d_{BP}/d_0 \qquad (2)$$

The refractive index was found to increase slightly on cooling from the isotropic liquid, as shown in Fig. 6. The dispersion of the refractive index of the blue phases is *ca.* 1.63–1.67, as also shown in Fig. 6.

Apart from a constant shift, the dispersion curves of the refractive index in the blue phase and the isotropic liquid phase are almost the same. The jump in the refractive index at the isotropic–blue phase transition was explained by the higher density of the blue phase compared to the isotropic liquid.[18]

For the AFM investigations we used a commercial TopoMetrix atomic force microscope in the non-contact mode[19] to obtain images of the surface modulation of the free surface of blue phase glasses. For large scans we used either the Explorer Tripot scanner (resolution: xy 100 μm–100 nm, z 12 μm–1 nm) or the Discoverer Tripot scanner (xy 24 μm–50 nm, z 12 μm–0.1 nm). Small scans were recorded using the Explorer Tube scanner (xy 2.5 μm–20 nm, z 0.8 nm). We always used pure Si-tips with Si-cantilevers (I-shaped, armlength 125 μm, resonance frequence 240–420 kHz) commercially available from Topometrix.

Results

On cooling the sample, blue fog BP_DIII appears immediately from the isotropic phase as dark, homogeneous blue regions of high optical activity. With decreasing temperature, the blue colour of the fog phase becomes brighter and exhibits strong fluctuations. The BP_DII-platelet texture grows very slowly from the discotic blue fog phase—due to the high viscosity—which indicates that supercooling of BP_DIII is possible. Using a slow cooling rate (about 0.5 K h^{-1}) large and well-defined BP_DII single crystals with a triangular morphology could be obtained from the blue fog [Fig. 7(*a*)]. The corresponding Kossel diagrams of these single crystals reveal a [111] orientation of a simple cubic structure with a spatial period of about 210±4 nm [Fig. 7(*b*),(*c*)]; the AFM image of the free surface in this region exhibits a periodical modulation with hexagonal symmetry [Fig. 7(*d*)]. The underlying lattice structure emerges much

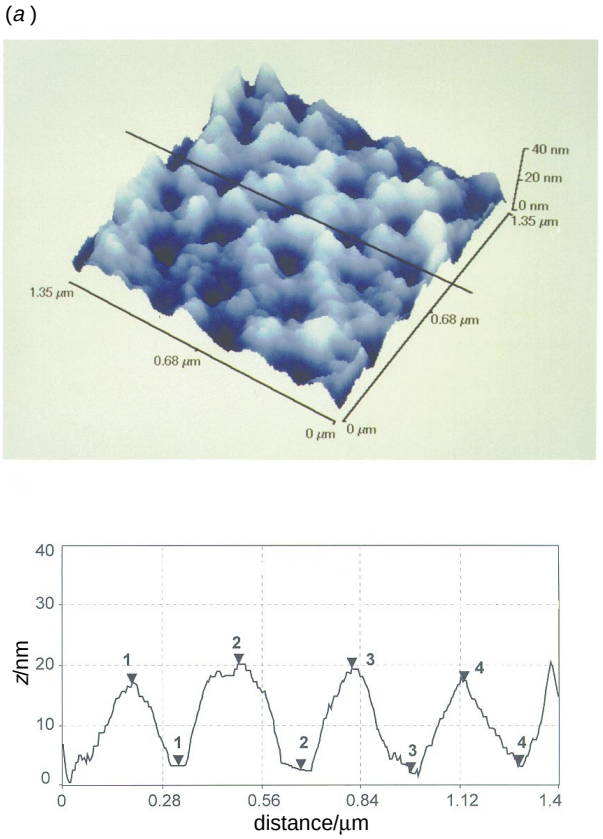

Fig. 8 (*a*) AFM image of the modulation altitude of the free surface in the region of a [111] orientated BP_DII single crystal. (*b*) The line measurement reveals an average modulation amplitude of about 15 nm (**1**: distance = 0.13 μm, height = 13.69 nm; **2**: distance = 0.17 μm, height = 17.89 nm; **3**: distance = 0.16 μm, height = 17.67 nm; **4**: distance = 0.15 μm, height = 14.27 nm).

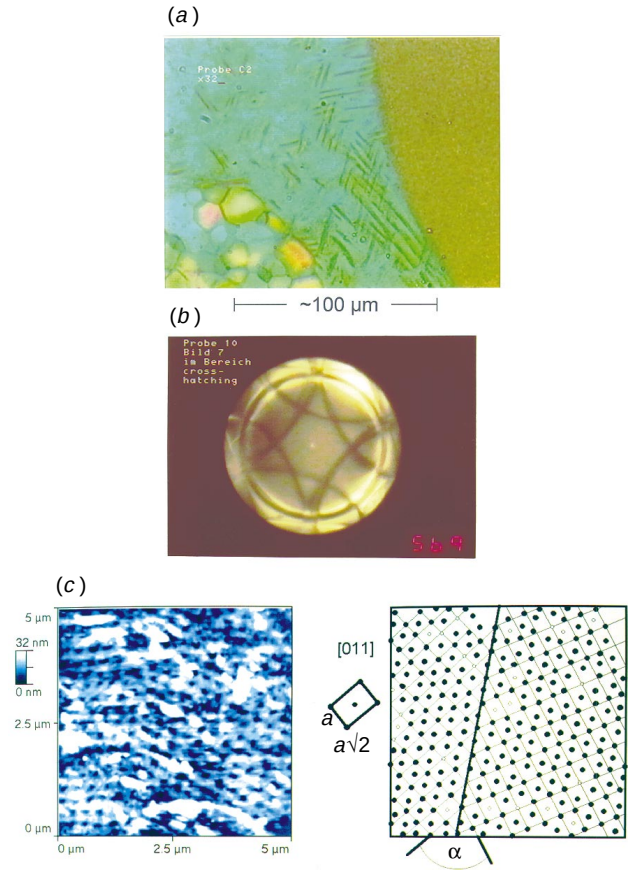

Fig. 9 (*a*) Optical micrograph of frozen BP_DI phase with cross hatching pattern after the transition from BP_DII, (*b*) the corresponding Kossel diagram in the region of cross hatching, and (*c*) both the AFM surface image in this region and a drawing of the lattice points as seen in this image. The lines indicates a grain boundary [$\alpha = 2\arcsin(1/\sqrt{3}) \approx 70.5°$].

more clearly in a drawing of the lattice points seen in this image [Fig. 7(*e*)]. From the AFM image the average lattice constant was determined in three directions to be 208 ± 8 nm, in fair agreement with the value obtained from the Kossel method.

As revealed by Kossel investigations of all samples, the BP_DII preferably grows in the [111] orientation. This is different from the observations of the BPII growth in calamitic systems, where BPII single crystals usually grow with the [100] axis perpendicular to the surface.[20] The modulation altitude of the surface of a 5–10 μm thick sample is shown in Fig. 8; it ranges from about 15 to 20 nm. This is quite large, and it is conceivable that the contraction of the blue phase during the cooling process contributes to the high surface modulation.

At the transition from BP_DII to BP_DI, a typical cross-hatching pattern appears on cooling [Fig. 9(*a*)]. The corresponding complex Kossel diagram [Fig. 9(*b*)] is a superposition of two diagrams resulting from two [011] body centred cubic structures, which meet at an angle of $2 \arcsin(1/\sqrt{3})$. This particular Kossel diagram was previously discussed by Pieranski *et al.*[21] In the AFM surface pattern in the cross hatching region, it is discernible that the surface periodicity is diagonally broken. A drawing of the lattice points seen in this image yields a twin structure in a [011] orientated body-centred cubic crystal, which coincides exactly with the Kossel diagram [Fig. 9(*c*)]. By the Kossel method a lattice constant of about 340 ± 5 nm is obtained, while the AFM images of the same sample give an average value of about 348 ± 15 nm.

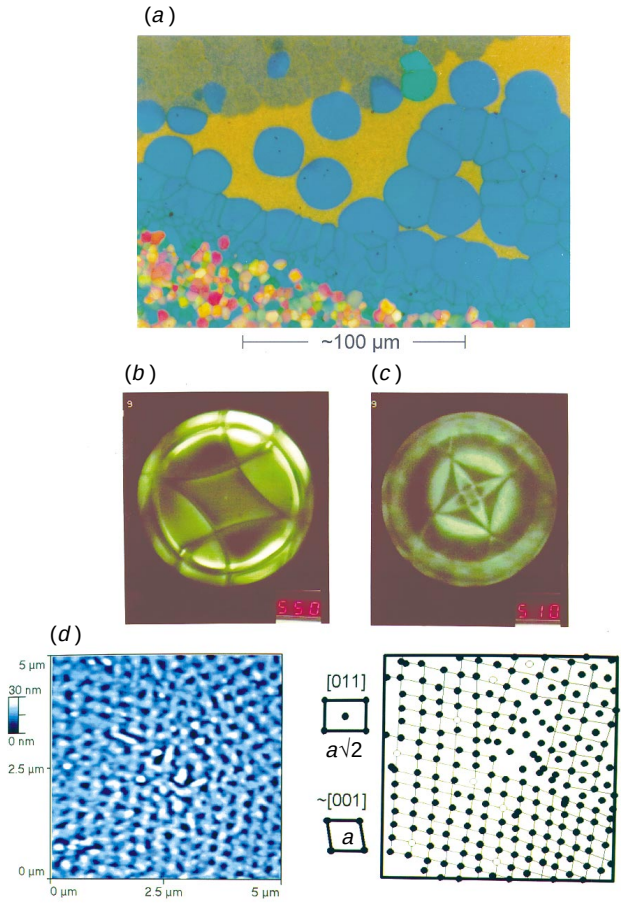

Fig. 10 (*a*) Optical micrograph of frozen BP_DI phase, Kossel diagram of a single crystal (*b*) in [011] orientation ($\lambda = 550$ nm) and (*c*) in [001] orientation ($\lambda = 510$ nm), and (*d*) the AFM surface pattern in the region of a phase boundary between a [001] orientation (left) and a [011] orientation (top right), plus a drawing of the lattice points seen in the AFM image (open cycles are regions covered by dust particles)

If the equilibration of the supercooled BP_DIII phase is performed in the BP_DI temperature range, BP_DI grows directly from the blue fog. In this case, no cross hatching pattern appears and the single crystals grow preferably in [011] orientation as shown by the Kossel diagram [Fig. 10(*b*)]. When the cooling process is not slow enough, other orientations of the body centred cubic BP_DI structure are observed [lower left corner in Fig. 10(*a*)] with some platelets in almost a [001] orientation [Fig. 10(*c*)]; the corresponding AFM image exhibits a periodic surface modulation with a phase boundary between the slightly distorted square symmetry of [001] orientated structure and the rectangular symmetry of [011] orientated BP_DI. The lattice constant of both orientations is again *ca.* 340 nm [Fig. 10(*d*)].

It is known for calamitic liquid crystals that the BPI modification can exhibit Grandjean–Cano lines in a wedge shaped preparation[22] as shown schematically in Fig. 11(*b*). By chance, we obtained a glassy sample of the discotic blue phase BP_DI in [011] orientation with a depression down to the substrate surface. Around this depression, the surface slopes considerably. The micrograph shows that the depression is surrounded by concentric lines [Fig. 11(*a*)]. One can suppose that they correspond to dislocation lines in the underlying cubic lattice resulting from the deformation due to the slanting sample surface. In this case we should find steps in the surface which should have a step height of about $(a/\sqrt{2})$ as shown in Fig. 11(*c*).

In the corresponding AFM image we indeed found a step like modulation of the free surface. The distance between these steps matches the line distance seen microscopically [Fig. 11(*a*)]. The average step height is about 230 nm which is in reasonable agreement with the value of 240 nm calculated from the lattice constant of BP_DI in the [011] orientation [Fig. 11(*d*)].

We carefully attempted to prepare samples of isotropic and

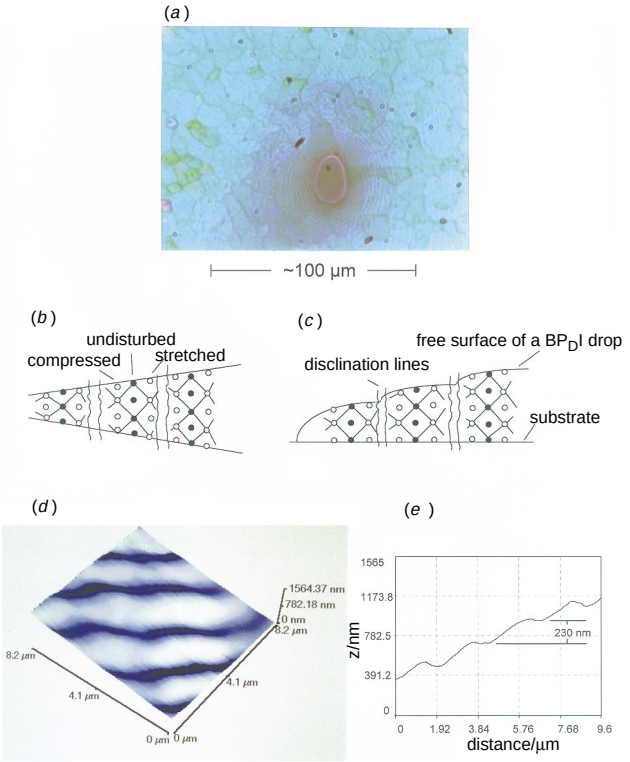

Fig. 11 (*a*) Texture of the frozen BP_DI in the [011] orientation with a crater-like surface depression down to the substrate, surrounded by concentric disclination lines. Sketch to explain the appearance of dislocation lines in the region of a sloping surface; (*b*) wedge shape preparation (ref. 22), (*c*) free surface. (*d*) AFM image and (*e*) line measurement showing a step like modulation of the free surface.

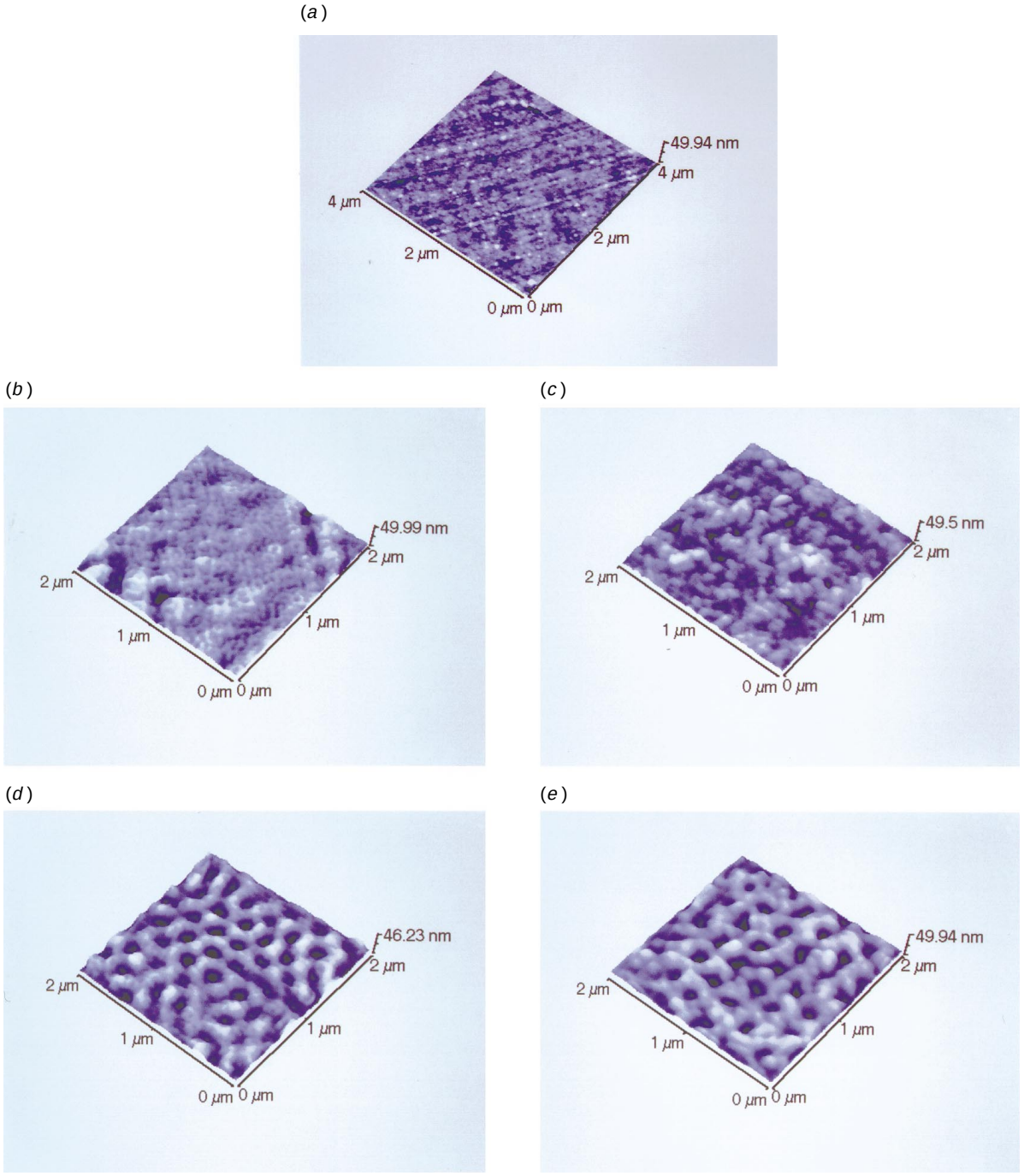

Fig. 12 AFM images of (*a*) free substrate and different glasses; (*b*) from the isotropic phase, (*c*) from the blue fog phase, (*d*) from BP_DII and (*e*) from BP_DI

BP_DIII glasses. In both cases the polarizing microscope showed a very delicately structured texture in the glass-like state, which was not seen in the isotropic liquid and BP_DIII phase themselves. Either the isotropic phase and the BP_DIII modification are not supercoolable, and we obtained unorientated cubic phases, or the structures obtained correspond to snapshots of the fluctuations in the isotropic liquid and in the BP_DIII.

AFM investigation on the glasses obtained from the isotropic phase of the chiral discotic mixture show a strongly modulated surface with randomly distributed dips. The distances between dips fluctuates from 65 to 75 nm and their average depth is about 8 nm [Fig. 12(*b*)]. The cause of the fine structure is not yet clear. Also, the free surfaces of glasses obtained from BP_DIII exhibit an irregular distribution of dips with a depth of about 11 nm, but in contrast to the isotropic glasses, the distances are 150–370 nm [Fig. 12(*c*)]. This seems to be in reasonable agreement with the results of previous light scattering experiments on a BPIII of similar pitch that showed a broad-band reflection of light with a maximum at 440 nm.[23] The light scattering indicates a short-range order with a basic period in the range of 200 nm.

Thus, the surfaces of the isotropic as well as the BP_DIII glasses exhibit only a random distribution of dips, while the surfaces of BP_DII and BP_DI single crystals show a periodic modulation over distances of several lattice periods [Fig. 12(*d*),(*e*)].

For comparison, the substrate surface was also investigated by atomic force microscopy. In the AFM image fine grooves are recognizable which probably result from the roll process during the manufacturing of the cover slides. The grooves are about 1 nm deep and their distances are irregular, otherwise the substrate surface appears flat [Fig. 11(*a*)]. As was expected,

the structure of the substrate surface is not displayed in the free surface of the frozen liquid crystalline sample.

In order to understand the details of the periodic relief observed for the blue phase samples one has to consider at least two effects. One is the influence of the boundary conditions at the free surface. At equilibrium, the relief will result from the competition between the surface energy and the bulk free energy. A theoretical discussion of this kind was presented recently[24] for the case of cholesteric phases, and the AFM images obtained for the glassy state of the investigated cholesteric oligomer are found to confirm the model. So far such theoretical descriptions have not been extended to the case of blue phases with their even more complicated bulk structure. However, it seems reasonable to assume that by fulfilling the boundary conditions at the free surface a partial smoothing out of details of the cubic blue phase structure takes place. It might be for this reason that more detailed reliefs reflecting the different molecular field structures which belong to arbitrary cuts through the complex cubic arrangements of double twist tubes and disclinations are not observed in the AFM images of the free surfaces.

A second very strong influence on the formation of a non-flat surface is anticipated from the thermal treatment of the sample. In particular, when cooling below the glass transition the thermal contraction might depend on the molecular orientation. To prove this effect we have performed AFM investigations on discotic cholesteric mixtures consisting of the same compounds with reduced concentration of the chiral component. By comparison with the textures observed by polarising microscopy, it is found that regions with homeotropic alignment are depressed and regions of planar alignment are elevated.[25]

Conclusion

While previous TEM and AFM studies on quenched blue phases in calamitic systems were made on microtome cuts,[14] this work reports the first AFM investigation on the free surface of frozen blue phases.

The glassy states of the discotic mixture under investigation are particularly suitable for atomic force microscopy. The combination of the Kossel method and atomic force microscopy proved to be very useful for structural studies of the blue phases and enables us to assign the observed topographies to the underlying lattice structures for BP_DI and BP_DII for different orientations.

With better resolution, a more detailed analysis of the director field seems possible, but this requires smoother surfaces, which might be achieved by a modified preparation technique of the sample.

The authors would like to thank Dr V. Vill for providing compound **1**. We also gratefully acknowledge to Professor Dr P. J. Collings as well as Dr H.-S. Kitzerow for helpful discussions and comments. This work was financially supported by the Deutsche Forschungsgemeinschaft (Sfb 335, Teilprojekt C5).

References

1 P. J. Collings, *Nature's Delicate Phase of Matter*, Adam Hilger IOP Publishing Ltd, Bristol, 1990, 196.
2 S. Meiboom, M. Sammon and D. W. Berreman, *Phys. Rev. A*, 1983, **28**, 3553.
3 H. Grebel, R. M. Hornreich and S. Shtrikman, *Phys. Rev. A*, 1984, **30**, 3264.
4 A. Saupe, *Mol. Cryst. Liq. Cryst*., 1969, **7**, 59.
5 D. K. Yang and P. P. Crooker, *Phys. Rev. A*, 1988, **35**, 4419.
6 P. P. Crooker and H.-S. Kitzerow, *Cond. Mater. News*, 1992, **1**, 6.
7 J. Thoen, *Phys. Rev. A*, 1988, **37**, 1754.
8 (*a*) Z. Kutnjak, C. W. Garland, C. G. Schatz, P. J. Collings, C. J. Booth and J. W. Goodby, *Phys. Rev. E*, 1996, **53**, 4955; (*b*) Z. Kutnjak, C. W. Garland, J. L. Passmore and P. J. Collings, *Phys. Rev. Lett*., 1995, **74**, 4859; (*c*) J. B. Becker and P. J. Collings, *Mol. Cryst. Liq. Cryst*., 1995, **265**, 163.
9 T. C. Lubensky and H. Stark, *Phys. Rev. E*, 1996, **53**, 714.
10 J. A. Zasadzinski, S. Meiboom, M. J. Sammon and D. W. Berreman, *Phys. Rev. Lett*., 1986, **57**, 364.
11 D. Krüerke, Kitzerow, G. Heppke and V. Vill, *Ber. Bunsenges. Phys. Chem*., 1993, **97**, 1371.
12 E. Dubois-Violette and B. Pansu, *Mol. Cryst. Liq. Cryst*., 1988, **165**, 151.
13 H.-S. Kitzerow, H. Schmid, A. Ranft, G. Heppke and R. A. M. Hikmet and J. Lub, *Liq. Cryst*., 1993, **14**, 911.
14 H. Dumoulin, P. Pieranski, H. Delacroix, I. Erk, J.-M. Gilli and Y. Lansac, *Mol. Cryst. Liq. Cryst*., 1995, **262**, 221.
15 S. Chandrasekhar, *Rep. Prog. Phys*., 1990, **53**, 57.
16 B. Kohne and K. Praefcke, *Chimia*, 1987, **41**, 196.
17 R. J. Miller and H. F. Gleeson, *J. Phys. II Fr*., 1996, **6**, 909.
18 K. Bergmann and H. Stegemeyer, *Ber. Bunsenges. Phys. Chem*., 1978, **82**, 1309.
19 R. Wiesendanger, *Jpn. J. Appl. Phys*., 1995, **34**, 3388.
20 H. Stegemeyer, Th. Blümel, K. Hiltrop, H. Onusseit and F. Porsch, *Liq. Cryst*., 1986, **1**, 3.
21 P. Pieranski, E. Dubois-Violette, F. Rothen and L. Strzelecki, *J. Physique*, 1981, **42**, 53.
22 Th. Blümel and H. Stegemeyer, *Liq. Cryst*., 1988, **3**, 195.
23 (*a*) E. I. Demikhov, V. K. Dolganov and S. P. Krylova, *Soc. Phys. JETP*, 1987, **66**, 998; (*b*) H.-S. Kitzerow, P. P. Crooker and G. Heppke, *Phys. Rev. Lett*., 1991, **67**, 2151.
24 R. Meister, H. Dumoulin, M.-A. Hallé and P. Pieranski, *J. Phys. II Fr*., 1996, **6**, 827.
25 A. Saupe, A. Hauser, M. Thieme, G. Heppke and D. Krüerke, *Liq. Cryst*., in the press.

Paper 7/03272B; *Received* 12*th May*, 1997